Practical Demonstration of RGC and Modified RGC TIAs for VLC systems

Amany Kassem and Izzat Darwazeh
Department of Electronic and Electrical Engineering, University College London, London, United Kingdom
Email: amany.kassem.15@ucl.ac.uk,i.darwazeh@ucl.ac.uk

***Abstract*—This work reports a modified regulated cascode (RGC) transimpedance amplifier (TIA) with tolerance to the ultra-high photodiode capacitances encountered in visible light communication systems. The new design is proposed to ameliorate internal miller capacitance limiting effects, inherent in traditional RGC designs through the use of a cascode circuit within the RGC. The paper introduces the design principle of the proposed RGC and presents derivation of tractable mathematical equations for describing the operation. The bandwidth advantage of the new design is shown through comparing the operation of the modified circuit to the traditional one using full circuit simulations. The paper presents full circuit designs, based on discrete components and printed circuit board (PCB) construction of both circuits and contrasts their operation, experimentally demonstrating bandwidth advantage for different values of photodiode capacitances and amplifier transimpedance gain values. Measurements show that using the modified RGC TIA results in a bandwidth improvement of over 200 % relative to the conventional RGC design, achieving a bandwidth of 200 MHz at 2 KΩ transimpedance gain with a 300 pF photodiode capacitance. As such, this is one of the highest bandwidths reported for such high capacitances, to-date.**

***Index Terms*—Optical receiver, regulated cascode, transimpedance amplifier, visible light communication**

I. Introduction

In visible light communications (VLC), achieving high data rates is a major challenge due to the limitations imposed by the opto-electronic devices of the transmitter (light emitting diodes (LEDs) have limited bandwidth and optical power) and the receiver (photoactive area, gain and bandwidth trade-off in photodiodes) [1, 2]. To combat such limitations to achieving high transmissions speeds, researchers have proposed the use of several techniques including bandwidth enhancement through the design of optimised analogue circuits. Such as the use of optically lossless equalisers to ameliorate the bandwidth limiting capacitances in LEDs as in [3] and the use of transimpedance amplifiers (TIAs) with high tolerance to large photodiode junction capacitance C_{pd} as in [4–6]. Furthermore, the use of advanced modulation formats [7–9] and other digital signal processing techniques to improve the utilisation of the available system bandwidth.

At the receiver, the challenge is to capture sufficient amount of light to ensure correct detection of the transmitted information and maximise the signal to noise ratio (SNR). This is a difficult challenge due to two reasons; first, the nature of the free space channel, whose loss is proportional to the square of the transmission distance, becomes prohibitive for practical distances. Second, the majority of photodiodes used in VLC systems are made of silicon, which has poor responsivity in the visible light frequency range, especially at the blue wavelengths commonly used in VLC. To boost the received optical power and maximise the associated photocurrent, especially for applications that demand large transmission distances, ideally the receiver should have a large area photodiode to maximise light capture. Alternatively, systems may employ high gain TIAs to convert the low amplitude photocurrent from the photodiode into an amplified voltage. Ideally, systems would combine both large photo active area detectors and high gain TIAs [10].

Large area photodiodes have highly limited bandwidths, particularly when followed by either 50-Ω or high impedance TIAs, such limitation arises from their substantially high C_{pd}. In the vast majority of VLC reports [7, 8], such bandwidth limitation is avoided by employing small area photodiodes, which are simply incapable of collecting sufficient optical power to allow practical distances.

Using low input impedance TIAs configuration is advantageous in tolerating high C_{pd}. This is because the dominant time constant, which determines the receiver bandwidth, is a product of photodiode capacitance and the TIA input resistance. Hence, a TIA with low input resistance reduces the time constant and significantly increases the bandwidth. Circuits with ultra-low input resistance, such as the common base (CB) [11] TIA and the regulated cascode (RGC) [12], originally proposed for older generations of optical fibre communication systems, are more recently found to be highly attractive for use in VLC systems [4, 5, 13–15].

Our work in [5] proposed the use of a modified RGC TIA that treat some of its inherent bandwidth limitations to enhance its tolerance to exceptionally high C_{pd}. In this work, we describe a simplified model analysis of the RGC and modified RGC TIAs based on hybrid-π models. We demonstrate both the RGC and modified RGC TIAs using discrete components. Measurements of the modfied RGC shows a bandwidth improvement of 200% in comparison to the conventional RGC configuration at C_{pd} equals 300 pF and up to 600 pF; to the best of our knowledge, these are the best results reported for such high values of photodiode capacitance. The TIAs bandwidth performance is examined while varying some design parameters such transimpedance gain and transistor currents. The proposed modified RGC demonstrates bandwidth insensitivity to transimpedance gain variations. Such attractive

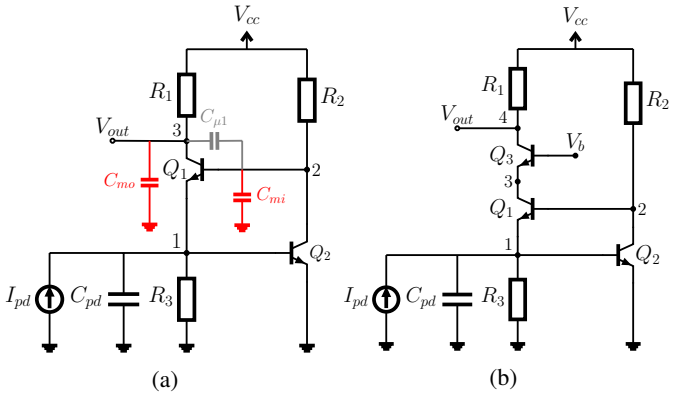

Fig. 1: Circuit diagram for (a) RGC (b) Modified RGC

feature will be valuable in enhancing the flexibility of VLC receivers, since employing automatic gain control (AGC) is normally desirable due to the variety of received signal powers dictated by the distance [10].

II. Design of the Transimpedance Amplifier

A. Conventional RGC

The conventional RGC configuration in Fig. 1a is widely described as a modification to the common base (CB) stage (Q_1) with feedback presented by a common-emitter (CE) stage (Q_2). this has the benefit of reducing the input resistance by a factor approximately equals the voltage gain of the CE. Interestingly, when inspecting the signal flow in Fig. 1a, it is clear (although counter-intuitive) that through the feedback path, the signal flowing from the collector of Q_2 into the base of Q_1, sees Q_1 as a CE instead of a CB stage, since Q_2 feeds the base of Q_1, which in turn outputs a voltage signal at its own collector. Hence, the feed back signal, now present at the base of Q_1, experiences its base collector capacitance $C_{\mu 1}$ as a Miller capacitance at the collector of Q_1, and more significantly at the base of Q_1. This Miller capacitance interplays with the large photodiode capacitance C_{pd} to generate a complex pole at the input that dictates the bandwidth of the RGC. Detailed pole-zero analysis of this circuit was reported by the authors in [5].

To investigate the effect of this Miller capacitance, we apply nodal analysis to the simplified equivalent model of the RGC shown in Fig. 2a. The model was simplified to obtain a compact and tractable RGC transfer function, by applying Miller theorem to split $C_{\mu 1}$ into its Miller equivalent capacitances at the base and collector of Q_1, namely C_{mi} and C_{mo}, respectively. Where $C_{mo} \approx C_{\mu 1}$ and C_{mi} approximately equals the product of $C_{\mu 1}$ and the voltage gain of Q_1 ($C_{\mu 1} g_{m1} R_1$). Hence, the RGC input resistance can be expressed by:

$$R_{in} = \frac{1}{g_{m1}(1 + g_{m2} R_2)} \tag{1}$$

Where g_{m1} and g_{m2} are Q_1 and Q_2 transconductance and R_2 are the load resistor for Q_2.

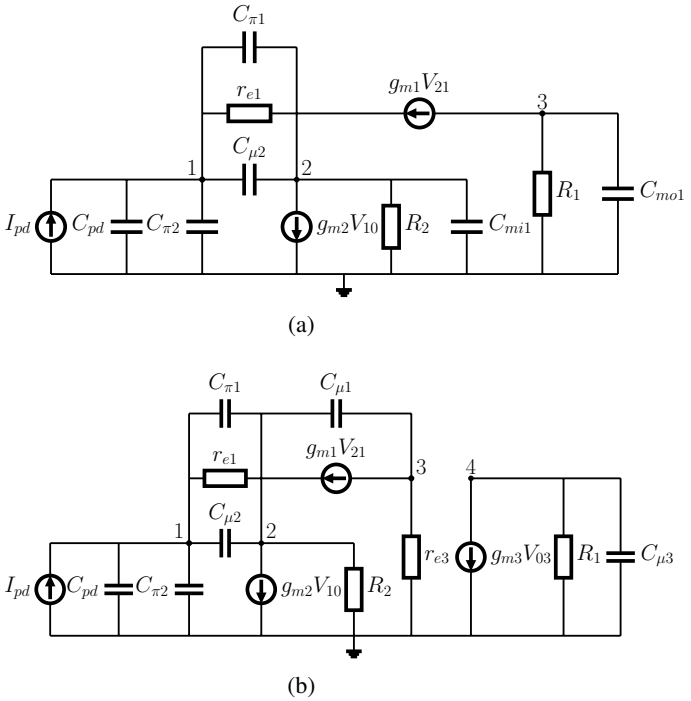

Fig. 2: Simplified equivalent model of (a) RGC (b) Modified RGC

The RGC transimpedance gain (A_T) is approximately given by a transfer function consisting of a complex input pole $\omega_{p(1,2)}$ and a real output pole ω_{p3}, derived to be:

$$A_T = R_T \frac{1}{[1 + s/\omega_n Q + s^2/\omega_n^2][1 + s/\omega_{p3}]} \tag{2}$$

Where

$$R_T = R_1 \tag{3}$$

$$\omega_n = \sqrt{\frac{g_{m1}(1 + g_{m2} R_2)}{R_2(C_{in} C_t + C_{in} C_{mi} + C_t C_{mi})}} \tag{4}$$

$$Q = \frac{\sqrt{g_{m1} R_2 (1 + g_{m2} R_2)(C_{in} C_t + C_{in} C_{mi} + C_t C_{mi})}}{C_{in} + C_t(1 + g_{m2} R_2) + g_{m1} R_2 C_{mi}} \tag{5}$$

ω_n and Q are the natural frequency and Q-factor of $\omega_{(p1,2)}$. Whereas $\omega_{(p1,2)}$ and ω_{p3} are given by:

$$\omega_{p(1,2)} = \frac{\omega_n}{2Q} + \omega_n \sqrt{1 - 4Q^4} \tag{6}$$

$$\omega_{p3} = \frac{1}{R_1 C_{mo}} \tag{7}$$

Where $C_{in} = C_{pd} + C_{\pi 2}$ and $C_t = C_{\pi 1} + C_{\mu 2}$, at which $C_{\pi 1}$ and $C_{\pi 2}$ are the base emitter capacitances of Q_1 and Q_2. The frequency behaviour of the transimpedance gain will be dictated by the interaction of the complex and real poles. The complex pole is largely dominant, except for high values of transimpedance gains (large values of R_1). Equations (4)-(6) show that the Miller effect limits the frequency of the complex pole $\omega_{p(1,2)}$.

B. Modified RGC

The above study of the RGC indicates a major limitation on bandwidth and transimpedance gain imposed by C_{mi}. Since increasing R_1 to boost the RGC transimpedance gain, have the undesirable effect of increasing C_{mi}, hence, significantly reducing the bandwidth and therefore imposing a stringent trade-off between transimpedance gain and bandwidth. Furthermore, increasing g_{m1} to extend the RGC bandwidth by reducing the input resistance also have the counteractive effect of increasing C_{mi}, hence, limiting the achievable bandwidth enhancement.

Such impact on the RGC bandwidth, as a result of increasing C_{mi} via either R_1 or g_{m1}, is made clear from (4), where C_{mi} appears in the denominator of ω_n. The capacitances C_{pd} and C_{mi} are the dominant capacitances and are therefore the root cause of the bandwidth limitation. Therefore, high values of C_{mi} would clearly reduce the frequency of ω_n and therefore the complex pole frequency dictating the bandwidth. Hence, if C_{mi} is omitted by neutralising the Miller effect, eliminating the C_{mi} term in (4), then the frequency of ω_n can be significantly increased as g_{m1} increases with the direct result of increasing the RGC bandwidth. Advantageously, the complex pole frequency becomes independent of the value of R_1, which would result in the bandwidth being far less dependent on changes in transimpedance gain. As such the gain can be increased whilst largely maintaining the desirable high bandwidth.

The Cascode configuration has been used for many years due to its advantageous characteristics in neutralising the Miller effect, mainly in CE amplifiers [16]. Fig. 1b shows the modified RGC TIA. In this circuit the Miller capacitance resulting from $C_{\mu 1}$ of Q_1 is eliminated through a cascode configuration that adds a CB stage Q_3. Therefore, the signal flowing from the collector of Q_2 to the base of Q_1 is not limited by the Miller effect of $C_{\mu 1}$. In other words, the proposed RGC modification extends the bandwidth of the RGC by neutralising the impact of the Miller capacitance on the frequency of $\omega_{p(1,2)}$, thus shifting the location of the $\omega_{p(1,2)}$ to a higher frequency.

By conducting similar nodal analysis to the simplified equivalent model of the modified RGC shown by Fig. 2b, we obtain the modified RGC input resistance as given by (1). Furthermore, the modified RGC can be described by transfer function as given by (2), where the DC transimpedance gain remains same as given by (3). However, the frequency $\omega_{p(1,2)}$ is now defined by ω_n and Q as:

$$\omega_n = \sqrt{\frac{g_{m1}(1+g_{m2}R_2)}{R_2(C_{in}(C_t+2C_{\mu 1})+C_tC_{\mu 1})}} \tag{8}$$

$$Q = \frac{\sqrt{g_{m1}R_2(1+g_{m2}R_2)(C_{in}(C_t+2C_{\mu 1})+C_tC_{\mu 1})}}{C_{in}+(C_t+C_{\mu 1})(1+g_{m2}R_2)+C_{\mu 1}g_{m1}R_2} \tag{9}$$

The output pole ω_{p3} is given by:

$$\omega_{p3} = \frac{1}{R_1C_{\mu 3}} \tag{10}$$

It can be seen clearly from (8) and (9) that the C_{mi} term of (4) and (5) is now removed, therefore, the frequency of the dominant input complex pole $\omega_{p(1,2)}$ of the modified RGC is increased, resulting in significant bandwidth extension. Furthermore, $\omega_{p(1,2)}$ is no longer a function of R_1. Thereby, in theory, the bandwidth of this circuit is independent of its transimpedance gain when the frequency spacing between $\omega_{p(1,2)}$ and ω_{p3} is sufficiently large. Such bandwidth behaviour is illustrated by recording the bandwidth of the RGC and modified RGC while varying the transimpedance gain (R_1). The two TIAs are simulated using silicon NPN transistors BFU520A (f_T= 10 GHz) at bias currents I_{C1}= 1 mA and I_{C2}= 2 mA, while R_1 is varied from 200 Ω to 2 kΩ. Full circuit models are used for the transistors and ideal passive models are assumed. Fig. 3 shows the simulated 3-dB bandwidths of the two TIAs versus transimpedance gain. Noticeably, the modified RGC exhibits little variation in its bandwidth as R_1 (transimpedance gain) is increased; a decade increase in gain results in less than 20% bandwidth reduction. This is because the dominant $\omega_{p(1,2)}$ is independent of R_1. Nevertheless, the slight reduction in the modified RGC bandwidth at higher R_1 values (800 Ω and above) is due the reduction in the frequency of ω_{p3}, which reduces the pole spacing between $\omega_{p(1,2)}$ and ω_{p3}, as such making the effect of ω_{p3} more significant. This is contrasted to the case of the conventional RGC, where we observe substantial reduction in the bandwidth as R_1 is increased. Whereas, its bandwidth at 2 kΩ is approximately reduced by over 60 % in comparison to its value at 200 Ω. Hence, the modified RGC offers a significant improvement in both bandwidth and transimpedance gain. This advantageously allows higher detected powers and better SNR ratios, which is a fundamental requirement to enable high data rates long-span VLC links.

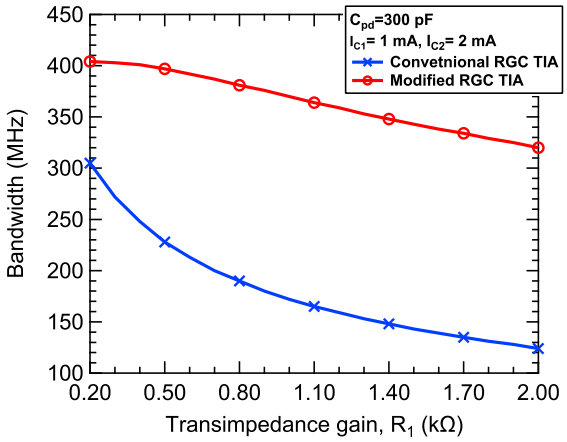

Fig. 3: Bandwidth variation of the RGC versus the modified RGC as the transimpedance gain (R_1) is increased

III. Comparative Assessment of the TIAs

Using discrete components, the two TIAs described above were built and tested, each with the addition of an output buffer- common collector (CC) stage, designed to provide 50-Ω output matching. Fig. 4 shows the fabricated FR4

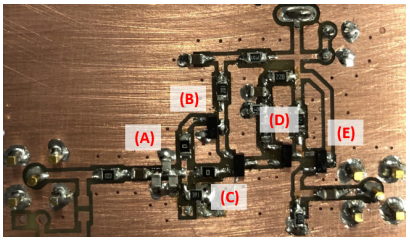

Fig. 4: Fabricated Modified RGC TIA PCB (A) PD model (B) CE (Q_2) stage (C) CB (Q_1) stage (D) CB (Q_3) stage (E) Additional CC stage

double-sided printed circuit board (PCB) of the modified RGC TIA. The PCB is populated using silicon NPN transistors BFU520A (f_T = 10 GHz) and with surface mount devices (SMD) used for all resistors and capacitors.

To test the performance of the TIAs , first, the scattering parameters of the fabricated RGC and modified RGC TIA are measured using a vector network analyzer (VNA). These are then converted into corresponding impedance parameters to obtain the transimpedance gain responses. To facilitate the study and measurements at exact capacitance values, the photodiode is modelled by inserting a series 1 kΩ resistor to convert the VNA voltage into current, analogous to the photodiode current. Whereas, C_{pd} is modelled as a shunt input capacitance equals 300 pF. The measured results are compared to simulation results, where the simulated results is based on post PCB layout. The simulation takes into account the effect of a) PCB parasitic effects, b) input transmission lines and c) input capacitor models.

Noting that using such large values of surface mount capacitors to represent the photodiode capacitance imposes severe limitation in demonstrating the full bandwidth advantage of the modified RGC in measurements. This is because of the low self resonance frequency associated with such high value of surface mount capacitors. This low self resonance frequency interferes with the amplifier frequency response, hence limiting the demonstrated bandwidth enhancement that could be achieved by the modified RGC. Nevertheless, such measurement limitation is not prevalent if the modified RGC TIA were to be measured optically with a large area photodiode. Even so, the following set of measurements still shows the advantage of the modified RGC over the conventional design.

To demonstrate the bandwidth insensitivity of the modified RGC to transimpedance gain variations in comparison to the conventional RGC. The transimpedance gain responses of the two TIAs is measured while increasing R_1 in the range of 240 Ω to 2 kΩ. Recalling, the transimpedance gain of the two TIAs equals R_1 as given by (3). Figs. 5a and 5b shows the measured and simulated transimpedance gain responses of the RGC and modified RGC for each respective DC transimpedance gain at a fixed C_{pd}= 300 pF, I_{C1}= 1 mA and I_{C2}= 2 mA. From Fig. 5a, it can be seen that measurements are in a good agreement with simulations. Moreover, it can be clearly seen that the bandwidth of the RGC drops to less than 30

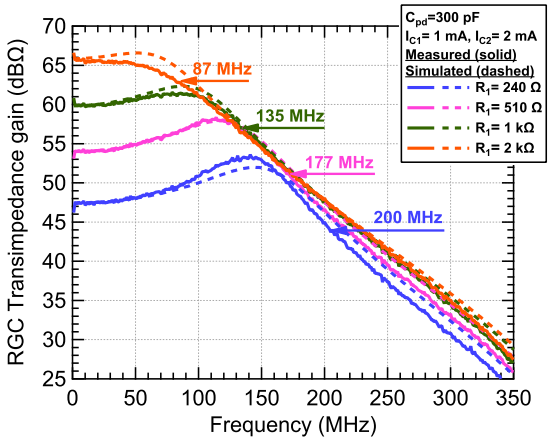

(a)

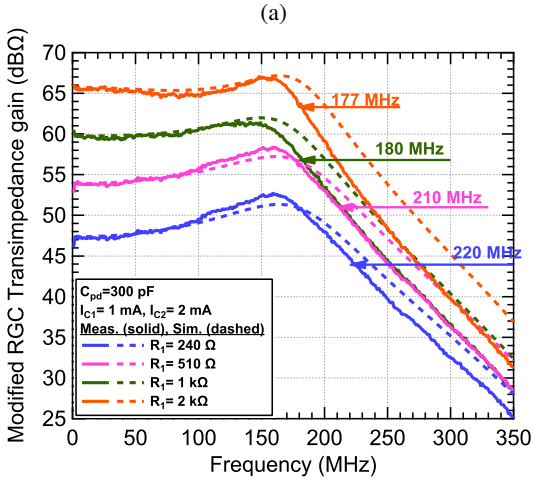

(b)

Fig. 5: Measured and simulated frequency responses for varying transimpedance gain at C_{pd}= 300 pF (a) RGC (b) Modified RGC

% of its value as the transimpedance gain increases from 240 Ω (47.6 dbΩ) to 2 kΩ (66 dbΩ). This substantial drop in bandwidth is mainly because the dominant input complex pole $\omega_{p(1,2)}$ is a function of R_1 as imposed by the Miller capacitance C_{mi} associated with $C_{\mu 1}$, as indicated by (4). In other words, increasing R_1 has the direct effect of increasing the Miller multiplier $g_{m1}R_1$ of $C_{\mu 1}$, hence reducing the frequency of ω_n and in turn the frequency of the dominant $\omega_{p(1,2)}$ dictating the RGC bandwidth. Therefore, imposing a trade-off between bandwidth and transimpedance gain. It is worth noting that similar bandwidth limiting effect is imposed by C_{mi}, when attempting to enhance the RGC bandwidth by reducing the input resistance via increasing g_{m1}, which in turn increase C_{mi}. Hence, limiting the RGC achievable bandwidth extension. Nevertheless, such effects are not shown, since it is generally not preferable to increase g_{m1} as it could potentially limit the achievable transimpedance gain, due to associated increase the voltage drop across R_1, hence requiring higher voltage supplies V_{cc} in order to maintain the bias conditions for

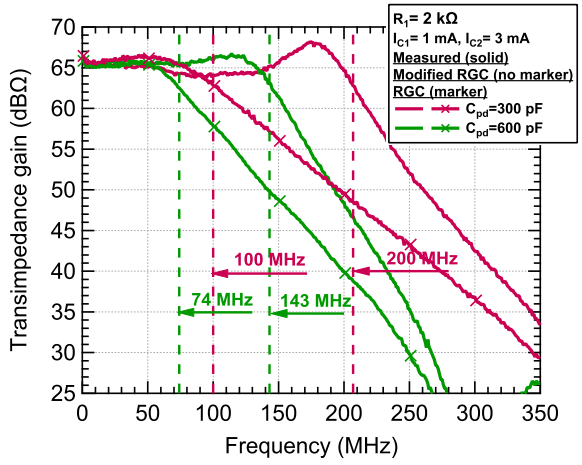

Fig. 6: Measured frequency responses of the RGC versus Modified RGC for varying C_{pd} at 2 kΩ transimpedance gain

Q_1. Nevertheless, the effects of increasing g_{m1} were studied in detail [5].

In contrast to the behaviour observed for the modified RGC TIA shown in Fig. 5b, where clearly the TIA exhibits bandwidth behaviour that is almost independent of its transimpedance gain, which confirms the bandwidth advantage of ameliorating the inherent Miller capacitance C_{mi} of the conventional RGC as suggested by the mathematical analysis conducted earlier. The bandwidth reduction of the modified RGC, as a result of increasing its transimpedance gain by almost one order of magnitude from 240 Ω to 2 kΩ, is less than 30%, which is almost negligible in comparison to the substantial increase in the transimpedance gain. Furthermore, it is verified that such minimal bandwidth reduction is largely due to bandwidth limitations resulting from the additional output buffer and its interaction with other circuit elements. Hence, if the output CC stage is further optimised then the modified RGC bandwidth should, in theory, be constantly maintained.

Therefore, it can be concluded that the modified RGC offers substantial bandwidth enhancement in comparison to the conventional RGC design, especially at high transimpedance gains as a result of neutralising the Miller effect of $C_{\mu 1}$. In addition, having insensitive bandwidth performance with increasing transimpedance gain, which is particularly valuable in the application of VLC where high gain and bandwidth are of utmost importance. Notwithstanding, such behaviour is only maintained to an extent where the output pole ω_{p3} is sufficiently higher than $\omega_{p(1,2)}$. Recalling, ω_{p3} is a function of R_1 as given by (10), which dictates the transimpedance gain. Hence, in such case attempting to increase the transimpedance gain (beyond 2 kΩ in the examples used in this work) would result in gradual reduction in the bandwidth performance, since the frequency of ω_{p3} becomes closer to the frequency of $\omega_{p(1,2)}$ and therefore, would have considerable impact on the bandwidth performance.

The bandwidth tolerance of the two TIAs to increasing C_{pd} is also examined by measuring the frequency responses at transimpedance gain equals 2 kΩ, I_{C1}= 1 mA and I_{C2}= 3 mA for C_{pd} equals 300 pF and 600 pF as shown by Fig. 6. Clearly, for C_{pd}= 300 pF, it can be seen that the modified RGC achieves a bandwidth extension of almost 200 % in comparison to the conventional RGC with just slight increase in peaking. For the C_{pd}= 600 pF, similar bandwidth advantage is still maintained, achieving also a bandwidth extension of 200 % in comparison to the conventional RGC with a peaking amplitude of approximately 3 dB.

IV. Conclusion

In this paper, we report the design, analysis and experimental verification of a modified regulated cascode TIA proposed to eliminate the undesirable bandwidth limiting inherent Miller capacitance of the RGC CB stage. We show through mathematical analysis and measurements of the proposed RGC that by introducing a cascode stage a substantial improvement in bandwidth, transimpedance gain can be realised. Moreover, the newly proposed modified RGC exhibits an almost insensitive bandwidth performance with respect to increasing transimpedance gain. Experimental results show the advantage of the new design where the bandwidth is doubled relative to the traditional RGC and where the gain of the modified circuit can be increased by up to 18 dB with less than 30% loss in bandwidth. Bandwidth 200 MHz was measured when a 300 pF capacitance was used at the input of the TIA and for an overall transimpedance gain close to 2 kΩ; which is, to our best knowledge, the widest band ever reported at such high input capacitance. Overall the new design's merits will be advantageous in the application of large transmission distance VLC link, where large area photodiodes are required to collect enough optical signal whose photocurrent in turn requires higher levels of amplifications to generate reasonable SNR levels for appropriate signal detection.

Acknowledgment

This work was supported in part by Engineering and Physical Sciences Research Council (EPSRC) MARVEL under Grant EP/P006280/1.

References

[1] S. Rajbhandari, J. J. D. McKendry, J. Herrnsdorf, H. Chun, G. Faulkner, H. Haas, I. M. Watson, D. O'Brien, and M. D. Dawson, "A review of gallium nitride LEDs for multi-gigabit-per-second visible light data communications," *Semiconductor Science and Technology*, vol. 32, p. 023001, jan 2017.

[2] P. A. Haigh, *Visible Light*. IOP Publishing: Bristol, UK, 2020.

[3] A. Kassem and I. Darwazeh, "Use of negative impedance converters for bandwidth extension of optical transmitters," *IEEE Open Journal of Circuits and Systems*, vol. 2, pp. 101–112, 2021.

[4] B. Huang and H. Chen, "A monolithic optical receiver chip for free space visible light communication system," in *2012 IEEE 11th International Conference on Solid-State and Integrated Circuit Technology*, pp. 1–3, 2012.

[5] A. Kassem and I. Darwazeh, "A high bandwidth modified regulated cascode TIA for high capacitance photodiodes in VLC," in *2019 IEEE International Symposium on Circuits and Systems (ISCAS)*, pp. 1–5, 2019.

[6] J. L. Cura and L. N. Alves, "Bandwidth improvements in transimpedance amplifiers for visible-light receiver front-ends," in *2013 IEEE 20th International Conference on Electronics, Circuits, and Systems (ICECS)*, pp. 831–834, 2013.

[7] D. Tsonev, H. Chun, S. Rajbhandari, J. J. D. McKendry, S. Videv, E. Gu, M. Haji, S. Watson, A. E. Kelly, G. Faulkner, M. D. Dawson, H. Haas, and D. O'Brien, "A 3-Gb/s single-LED OFDM-based wireless VLC link using a gallium nitride μLED," *IEEE Photonics Technology Letters*, vol. 26, no. 7, pp. 637–640, 2014.

[8] P. Chvojka, P. A. Haigh, A. Minotto, A. Burton, P. Murto, Z. Genene, W. Mammo, M. R. Andersson, E. Wang, Z. Ghassemlooy, F. Cacialli, I. Darwazeh, and S. Zvanovec, "Expanded multiband super-nyquist CAP modulation for highly bandlimited organic visible light communications," *IEEE Systems Journal*, vol. 14, no. 2, pp. 2544–2550, 2020.

[9] P. Anthony Haigh and I. Darwazeh, "Visible light communications: Fast-orthogonal frequency division multiplexing in highly bandlimited conditions," in *2017 IEEE/CIC International Conference on Communications in China (ICCC Workshops)*, pp. 1–8, 2017.

[10] R. Aguiar, A. Tavares, J. Cura, E. De Vaaconcelos, L. Alves, R. Valadas, and D. Santos, "Considerations on the design of transceivers for wireless optical LANs," in *IEEE Colloquium on Optical Wireless Communications*, pp. 2/1–231, 1999.

[11] B. Wilson and I. Darwazeh, "Low input resistance transimpedance optical preamplifier for fibre optic local area networks," in *1988., IEEE International Symposium on Circuits and Systems*, pp. 2531–2534 vol.3, 1988.

[12] S. M. Park and H.-J. Yoo, "1.25-Gb/s regulated cascode CMOS transimpedance amplifier for gigabit ethernet applications," *IEEE Journal of Solid-State Circuits*, vol. 39, no. 1, pp. 112–121, 2004.

[13] R. Y. Chen and Z.-Y. Yang, "CMOS transimpedance amplifier for gigabit-per-second optical wireless communications," *IEEE Transactions on Circuits and Systems II: Express Briefs*, vol. 63, no. 5, pp. 418–422, 2016.

[14] R. Y. Chen and Z.-Y. Yang, "CMOS transimpedance amplifier for visible light communications," *IEEE Transactions on Very Large Scale Integration (VLSI) Systems*, vol. 23, no. 11, 2015.

[15] E. S. Parapari, E. S. Parapari, and Z. D. Koozehkanani, "A broadband transimpedance amplifier (TIA) for visible light communication in 0.18 μm CMOS," in *2020 28th Iranian Conference on Electrical Engineering (ICEE)*, pp. 1–4, 2020.

[16] L. Moura and I. Darwazeh, *Introduction to linear circuit analysis and modelling: from DC to RF*. Elsevier, 2005.